JAERI-M
6685

# COMPARISON IN ELECTRON DENSITY DISTRIBUTION OF TOKAMAK PLASMA BETWEEN RUBY-LASER SCATTERING AND MILLI-METER WAVE INTERFEROMETRIC MEASUREMENTS

August 1976

T. MATOBA, A. FUNAHASHI, T. ITAGAKI,
K. TAKAHASHI, K. KUMAGAI and T. YAMAUCHI

日本原子力研究所
Japan Atomic Energy Research Institute

JAERI - M 6685

# Comparison in Electron Density Distribution of Tokamak Plasma Between Ruby-Laser Scattering and Milli-Meter Wave Interferometric Measurements

Tohru MATOBA[+], Akimasa FUNAHASHI, Tokiyoshi ITAGAKI[+],
Koki TAKAHASHI, Katsuaki KUMAGAI and Toshihiko YAMAUCHI

Division of Thermonuclear Fusion Research, Tokai, JAERI

( Received July 30 , 1976 )

The electron density in JFT-2 tokamak has been measured by two methods, i.e. Thomson scattering of ruby-laser light and interferometry of millimeter wave. Two-dimensional distribution of the scattered light intensities were obtained by scattering measurement ; absolute calibration was made by normalizing the scattered intensities with the averaged density determined from interferometric measurement. The horizontal density distributions in laser scattering were compared with those in from the averaged densities measured with a 4-mm interferometer through inverse-transformation. Agreement is good between the two measurements, except where they give erroneous data because of irreproducibility of the discharge.

---

+ ) Presently Division of Large Tokamak Development, Tokai, JAERI

# ルビーレーザ散乱およびミリ波干渉法によって測定されたトカマクプラズマの電子密度分布の比較

日本原子力研究所東海研究所核融合研究部

的場　徹[+]・船橋昭昌・板垣時良[+]
高橋興起・熊谷勝昭・山内俊彦

（1976年7月30日受理）

ＪＦＴ－２トカマクの電子密度を，ルビーレーザ光の散乱およびミリ波干渉法の２つの方法を使って測定した。散乱測定では，散乱光強度の２次元分布が得られ，散乱光の絶対強度較正は干渉測定法から求めた平均電子密度で規格化する方法で行った。ルビーレーザ散乱で測定した電子密度の水平分布を，４ミリ波干渉計で測定した平均密度を逆変換することによって得られた結果と比較した。これら２つの方法がプラズマ放電の非再現性のため正しい結果を与えない場合を除いては，これらの方法の間にはよい一致が見られた。

---

＋）　現在日本原子力研究所東海研究所大型トカマク開発部

CONTENTS

## 1. INTRODUCTION

In researches on high-temperature tokamak plasmas, it is of basic interest to have accurate knowledges of electron density distributions and the time evolutions. Two methods to measure the electron density in tokamaks have been mainly utilized. One is the scattering measurement of a ruby-laser light.[1] This method depends on the fact that the total intensities of electro-magnetic waves scattered from plasmas are proportional to the electron density at a local point, which is determined from an incident laser light and an observing direction on a scattered light. The other is the interferometry of electromagnetic waves which are ranging from milli-meter[2] to far-infrared[3] regions. The interferometric measurements, in principle, can determine the electron density averaged along a path of an electromagnetic wave transmitting through plasmas.

Although the laser scattering technique has a superior advantage which can permit one to measure the localized value of electron temperature and density, it is necessary to calibrate the scattered intensities to determine the absolute value of electron density. On the contrary the latter, interferometric measurements do not provide data with good spatial-resolutions but can rather easily present the absolute value of electron density. In many works on tokamak-researches, the scattered intensities are calibrated by cross-sections of Rayleigh scattering for molecular gases or by normalizing a spatial distribution of relative density along one direction by the fringe-shifts determined from interferometric measurements along the direction.

Present experiments provide recent experimental results of ruby-laser scattering measurements, in particular, on the distributions of electron density in JFT-2 tokamak-plasmas. Two-dimensional measurements on scattered intensities are performed with a ruby-laser scattering apparatus.[4] The electron density measured along a central, vertical path with a 4-mm wave interferometer is here used to calibrate the light intensities scattered from JFT-2 plasmas. In the interferometric measurements, horizontal distributions of electron density are determined from the averaged densities along different, eight vertical paths in the minor cross-section by using an inverse-transformation method. The purposes of the present report are to compare the horizontal distributions of electron density determined from scattering measurements with those from interferometric measurements and to present the justness of ruby-laser scattering

measurements on JFT-2 plasmas.

Figure 1 shows the plan view of JFT-2 tokamak-device[5] with various diagnostic apparatus. A ruby-laser scattering apparatus and 4-mm and 2-mm wave interferometers and used for the experiments described in the present report, and are positioned in the toroidal direction, as shown in the figure.

## 2. RUBY-LASER SCATTERING APPARATUS AND ITS MEASUREMENT

Figure 2 shows the schematic diagram of a ruby-laser scattering apparatus[4] for JAERI tokamak-devices. A ruby light is emitted from a Q-switched laser oscillator which has an energy of 5 -- 10 joules and a duration time of about 20 nanoseconds (i.e., output power 250 -- 500 MW). The ruby-laser light is irradiated vertically through a quartz window into JFT-2 device from down to top in the minor cross-section of the torus, and is focussed to 3 mm at the plasma center by a long-focal lens. The scattered light at 90 degrees to the irradiating beam is observed with a light collecting lens. The aperture ratio of the collecting lens is F 6.5. The observed point can be scanned horizontally and vertically with a periscope, in order to obtain spatial distributions in the minor cross-section. The scattered lights are analyzed in a 100 cm Czerney-Turner monochrometer (NIKON G-1000) and pass to twelve photomultipliers through an optical-transmitting system consisting of prisms and collimating lenses. Each photomultiplier detects the scattered light over the wavelength range of 70 Å, and is magnetically shielded with parmaloy co-axial tubes. The photomultiplier is RCA C31026, and has an ERMA III photocathode with rather flat spectral response in the wavelength range from 5000 Å to 7000 Å. The signals from photomultipliers are led to pre-amplifiers (40 db), delay-and-composite circuits and a high-speed oscilloscope. All measurements of the broadened profile in the scattered spectrum are performed at wavelength shorter than the ruby-laser wavelength (6943 Å).

Figure 3 presents details of the observation port (observation box) for ruby-laser scattering measurements. A laser beam can be chosen to pass along one of seven vertical light paths with a spacing of 6 cm. The 90-degrees, scattered lights are observed through a large rectangular quartz window, which is very convenient to obtain vertical distributions

in the whole minor cross-section. The laser beam dump and viewing dump are furnished to decrease stray lights. These dumps permit the stray lights to decrease down the levels, at the wavelength of 6943 Å, which are equivalent to the scattering from cold electrons at a density of $3 \times 10^{14}$ $cm^{-3}$. By considering a reduction of the stray lights in the monochrometer by the order of $10^{-4}$, the stray levels correspond an electron density of $10^{11}$ -- $10^{12}$ $cm^{-3}$ over the wavelength range observed in scattering measurements. In practical measurements, however, dominant noises are not due to the stray lights but originating from shot noises of photomultipliers. The levels of the shot noises do not permit one to determine the electron density less than $10^{12}$ $cm^{-3}$ for measurements on JFT-2 plasmas. Except when measurements are performed, these dumps and quartz windows are protected from metallisation due to plasma discharges with a shutter, as shown in the figure. Figure 4 summarizes main characteristics of the ruby-laser scattering apparatus for diagnoses of JAERI tokamaks.

The scattering apparatus has been in operation since fall 1973. Hitherto, many improvements were performed, for example, the intensification of magnetic shield to photomultipliers, utilization of gated integraters to increase ratio of signal to noise, usage of a helical flash lamp for an oscillator head to obtain good oscillated-patterns in incident lights, and addition of a subsidary shutter to the large observing window (for scattered lights) to reduce the metallisation.

Figures 5(a) and (b) show typical spectra of scattered signals observed in the center of plasma (X = 0, Z = 0). The operating conditions are also given in the figures. The obscissa is the channel number of photomultipliers, which is scaled proportionally to the square of the wavelength displacement from the central wavelength, $(\Delta\lambda)^2$. The ordinate in a logarithmic scale provides the scattered intensity calibrated absolutely according to the procedure which will be described in Section 4. The open circles in these figures represent the experimental data obtained from one shot of plasma discharge.

The scattering parameter $\alpha$ is much smaller than unity, and no co-operative features are to be expected for plasma parameters under the present experimental conditions. Therefore, a straight line in Fig. 5 indicates good evidence for the Maxwellian distribution of velocities transverse to the direction of toroidal magnetic field. The scattered profiles in a linear plot become a Gaussian shape, whose full half-width $\Delta\lambda_{1/2}$ is expressed by the following numerical equation;

$$\Delta\lambda_{1/2}(\text{Å}) = 32.2[T_e(\text{eV})]^{1/2} \quad (1)$$

with the electron temperature $T_e$ for 90 degrees, ruby-laser scattering measurements. The lines of a least-mean-square fit in scattered spectra give the electron temperatures of 667 ± 64 eV in Fig. 5(a) and 1170 ± 120 eV in Fig. 5(b) respectively.(*) The error widths of about 10 percents in temperature measurements are originating from shot noises of photo-multiplers.[7]

## 3. MEASUREMENTS OF MILLI-METER WAVE INTERFEROMETRY

A 4-mm wave interferometer is mainly used in the present experiments. The interferometer is a zebra-striped one, which is capable of producing five fringe-stripes and detecting down to one-tenth of one fringe-shift. It consists of a klystron (OKI-KA701, output 400 mW), microwave circuits, delay lines (total length 15 m), collecting lenses for 4-mm waves, and electronic circuits for producing zebra-stripes.

There are eight vertical paths for the interferometric measurements on JFT-2 plasmas, as shown in Fig. 6. The wave is transmitted into the plasmas through an aperture (3 cm in diameter) from top to down. An electric field of the wave is chosen to be parallel to the toroidal magnetic field. Quartz lenses for collecting 4-mm waves are attached to the apertures and simultaneously used to keep them vacuum-tight. Shutters are placed between the lenses and the plasmas to prevent the lenses from being opaque through metallisation due to plasma discharges.

Figure 7 presents a typical oscilloscopic traces of zebra-striped fringes measured along the central, vertical path X = 0 with a 4-mm interferometer. The relation between the electron density $n_e$ and observed fringe-shifts m is given by

$$\int n_e(z)dz(\text{cm}^{-2}) = \frac{2.24 \times 10^{13} \cdot m}{\lambda(\text{cm})} \quad (2)$$

(*) In determining these values of electron temperature, a correction due to the relativistic effect of electrons[6] is neglected. According to ref. 6c, the correction is negligibly small for temperatures less than 1000eV, about 5 percents for $T_e$ = 1200 eV, and 10 and 15 percents for $T_e$ = 1500 eV and 2000 eV respectively.

with the line element dz along the wave path and the wavelength $\lambda$ of electromagnetic wave. One fringe-shift in the figure is corresponding to the average electron density of $0.88 \times 10^{12}$ cm$^{-3}$. The maximum number of fringe shift is observed to be 14.3 at about 130 msec in the figure. The horizontal distribution of electron density is deduced from the averaged densities measured along the eight vertical-paths with a 4-mm wave interferometer, by assuming the shot-to-shot reproducibility of palsma discharge, and scanning the positions of a transmitting and a receiving horns horizontally.

A 2-mm wave interferometer is also used to measure the electron density averaged along the central, vertical path in the different toroidal position, as previously shown in Fig. 1.

## 4. CALIBRATION OF SCATTERED LIGHT INTENSITY

A power of the scattered light $W_s^{(o)}$ which is observed with a collecting lens is expressed by

$$W_s^{(o)} = \eta_{(o)} \cdot \frac{d\sigma_e}{d\Omega} \cdot n_e P_i dz d\Omega \tag{3}$$

with

$$P_i = \eta_{(i)} \cdot P_o \tag{4}$$

where $\eta_{(o)}$ is the transmission efficiency of the scattered light which transmits from an observed point to the collecting lens through an observing window, $\frac{d\sigma_e}{d\Omega}$ the differential cross-section of Thomson scattering per electron, $n_e$ the electron density at the observed point, $P_i$ the incident power at the observed point, dz and $d\Omega$ the irradiated length and the solid angle observed with the collecting lens. $\eta_{(i)}$ the transmission efficiency of an incident laser light, and $P_o$ the output power emitted from a ruby-laser oscillator. The value of $W_s^{(o)}$ is absolutely measured by calibrating the sensitivities of photomultipliers with a standard tangsten lamp. The laser power $P_o$ can be also determined from calorimetric measurements on the output energy. However, it is very difficult to evaluate the electron density from Eq. (3) and calibrated values of $W_s^{(o)}$ and $P_o$ because of some ambiguities in $\eta_{(o)}$ and $P_i$ (or $\eta_{(i)}$). Such an evaluation seems to provide erroneous densities, in particular, in measurements on

tokamak devices where there are some possibilities for the windows to be metallized.

Figure 8 illustrates the principle of density determination in Thomson scattering measurements. One method is to normalize the spatial distribution of apparent density $n_e^L(X, Z)$ determined from the calibrated values of $W_s^{(o)}$ and $P_o$ under the assumption of $\eta_{(o)} = 1$ and $\eta_{(i)} = 1$ by the average electron density $\bar{n}_e$ from interferometric measurements, i.e.,

$$\int_{-R}^{R} n_e(X,Z)dz = \gamma_e \int_{-R}^{R} n_e^L(X,Z)dz = \bar{n}_e(X) \int_{-R}^{R} dz \qquad (5)$$

where a compensation factor $\gamma_e$ is the correction due to the ambiguities in $\eta_{(o)}$ and $P_i$ and R is a radius of plasma boundary (i.e., the liner radius). The other method is an utilization of Rayleigh scattering, where the effective (laser) power $P_{eff} = \eta_{(o)} \cdot P_i$ is calibrated by comparing the value of $W_s^{(o)}$ with the light intensity of Rayleigh scattering from molecular gas fed in a vacuum chamber of plasma device. In this calibration, a compensation factor $\gamma_R$ is introduced by the relation

$$P_{eff} = \eta_{(o)} \cdot P_i = \eta_{(i)} \cdot \eta_{(o)} \cdot P_o = \gamma_R \cdot P_o \qquad (6)$$

If these two calibrations are performed with sufficient accuracy, it should be, of course, valid that $\gamma_e = \gamma_R$.

The present work adopts the former method. Figure 9 shows the horizontal distribution of electron density $\bar{n}_e(X)$ averaged along different vertical paths with a 4-mm wave interferometer (upper graph) and the vertical distribution of local apparent (uncompensated) density $n_e^L(0,Z)$ determined in a central vertical plane (X = 0) from scattering intensities (lower graph). In the figure X and Z refer to a horizontal and a vertical positions in the minor cross-section, the point of X = 0 and Z = 0 is the center of vacuum chamber (i.e., liner), the plus sign indicates the outer position or the upper position in the minor cross-section, R is the liner radius, and $\ell$ is the length of the microwave vertical path in the minor cross-section. From the figures, the compensation factor $\gamma_e$

$$\gamma_e = \frac{\bar{n}_e(0) \cdot \int_{-R}^{R} dz}{\int_{-R}^{R} n_e^L(0,Z)dz} \qquad (5')$$

is determined to be $\gamma_e = 4.1$.

## 5. COMPARISON OF ELECTRON DENSITY DISTRIBUTION

The lower graph of Fig. 10(a) provides the comparisons between the horizontal distributions of electron density determined from measurements on ruby-laser scattering (open circles with error bars) and 4-mm wave interferometry (solid curve). The values of electron density from scattering measurements are obtained by multiplying the apparent value $n_e^L(X, 0)$ measured in the equatorial plane (Z = 0) by the compensation factor $\gamma_e$ of 4.1. The horizontal distribution indicated by a solid curve is determined from the averaged densities $\bar{n}_e(X)$ by using an improved inverse-transformation method.[8] This result shows that satisfactory agreement between the horizontal distributions from these two methods is obtained. Another example is presented in Fig. 10(b), where the electron densities from scattering measurements are less than those from interferometric measurements by 15 -- 25 percents near the plasma center.

Figure 11 shows the examples of time-variations of plasma current and loop voltage. The operating condition is the toroidal magnetic field $B_t$ = 14 kG and peak plasma current $I_p^{(p)}$ = 100 kA. Figure 12 provides the time-variations of central electron temperature $T_{eL}$ determined from ruby-laser scattering measurements (upper graph) and of central density $n_e(0)$ from scattering measurements and average density $\bar{n}_e$ with 4-mm and 2-mm interferometers (lower graph). In Fig. 13 the central electron densities from scattering measurements (open circles with error bars) are compared with those from 4-mm wave interferometry (cross points) through an inverse-transformation. The different time-behaviours observed during 10 -- 25 msec may be originating from the irreproducibilities of plasma discharges. The observed discrepancy seems to be improved by multichannel interferometric measurements. The pulse-to-pulse variation of discharges during the interval was considerably larger than that after 25 msec, for example as shown in the lower graph of Fig. 12.

## 6. SUMMARY

In concluding the present report, we are going to summarize the results as follows;

(1) The distributions of electron density have been measured in JFT-2 tokamak by two methods, Thomson scattering of ruby-laser lights and interferometry of milli-meter waves.

(2) Two dimensional distributions of scattered intensities have been obtained in scattering measurements. In interferometric measurements the horizontal distributions of electron density have been determined through an inverse-transformation from eight vertically-averaged densities with a 4-mm wave interferometer.

(3) The scattered intensities observed in the central, vertical plane have been normalized by the averaged density determined from interferometric measurements along the plane. This calibration has shown that the compensation factor $\gamma_e$ defined by Eq. (5) equals to 4.1.

(4) Comparisons of horizontal density distributions between these two methods have been performed under various operating conditions.

(5) Fundamentally, good agreement between the two measurements has been found. However, some discrepancies have been observed, which may not be too large to be explained by scatters in the data of Thomson scattering or milli-meter wave measurements due to the irreproducibilities of plasma discharges.

(6) The central values of electron density have been accurately determined to be $(1.5 -- 2.5) \times 10^{13}$ cm$^{-3}$ from these two measurements in the present experiments.

## ACKNOWLEDGEMENTS

The authors are very grateful to Drs. N. Fujisawa, S. Konoshima and other members of JFT-2 and diagnostic groups for their helpful discussions and co-operation, and to S. Kunieda, N. Toyoshima and their groups for diligent efforts to the operation of JFT-2 device.

We also greatly appreciate their continuous encouragement performed by Drs. M. Tanaka and S. Mori.

REFERENCES

1a) M. J. Forrest et al.: Culham Report CLM-R-107 (July, 1970).

1b) M. Murakami et al.: ORNL-TM 4354 (September, 1973).

1c) D. Dimock et al.: MATT-906 (July, 1972),
D. Dimock et al.: Nuclear Fusion 13 (1973) 271.

1d) M. Charet et al.: EUR-CEA-FC-759 (February, 1975).

2a) E. P. Gorbunov: Proc. of the Second International Conference on Plasma Physics and Controlled Nuclear Fusion Research, Culham, UK, September, 1965 (IAEA, Vienna, 1966) vol. II, p.629.

2b) N. J. Grove et al.: MATT-813 (October, 1970).

3a) C. Etievant: EUR-CEA-FC-702 (Juin, 1973).

3b) Rh. Brossier and R. A. Blanken: EUR-CEA-FC-750 (May 1974).

3c) A. Nishizawa et al.: Japan J. Appl. Phys. (August, 1976 Issue).

4) T. Matoba et al.: JAERI-M 5515 (January, 1974, in Japanese).

5) N. Fujisawa et al.: Proc. of the Fifth International Conference on Plasma Physics and Controlled Nuclear Fusion Research, Tokyo, JAPAN, November 1974 (IAEA, Vienna, 1975) vol.I, p.3.

6a) R. E. Pechacek and A. W. Trivelpiece; Physics of Fluids 10 (1967) 1688.

6b) K. Hayase and T. Okuda: Institute of Plasma Physics (Nagoya University) Research Report, IPPJ-178 (October, 1973).

6c) M. Mattioli and R. Papoular: EUR-CEA-FC-732 (April 1974).

7) T. Itagaki et al.: JAERI-M 6476 (March, 1976, in Japanese).

8) T. Matoba and A. Funahashi: JAERI-M 6239 (September, 1975, in Japanese).

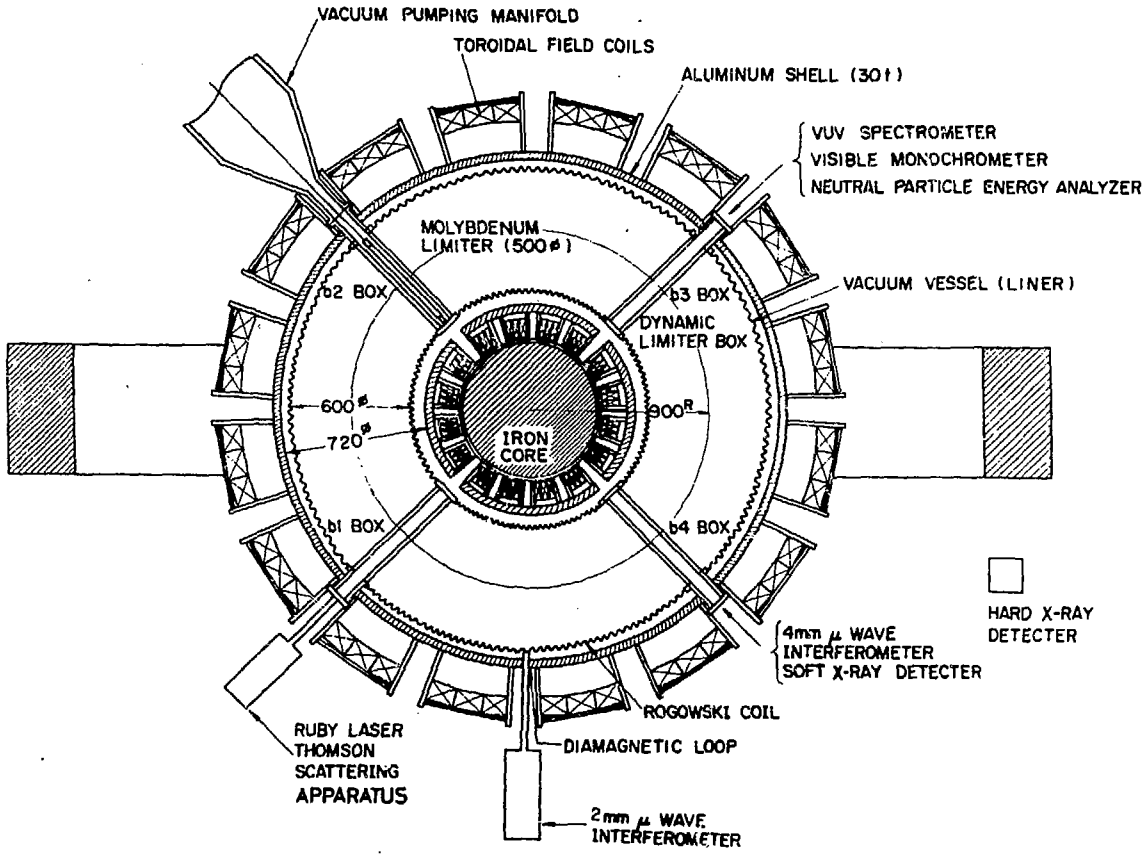


Fig. 1 JFT-2 tokamak device and diagnostic apparatus.[5)]



JAERI-M 6685

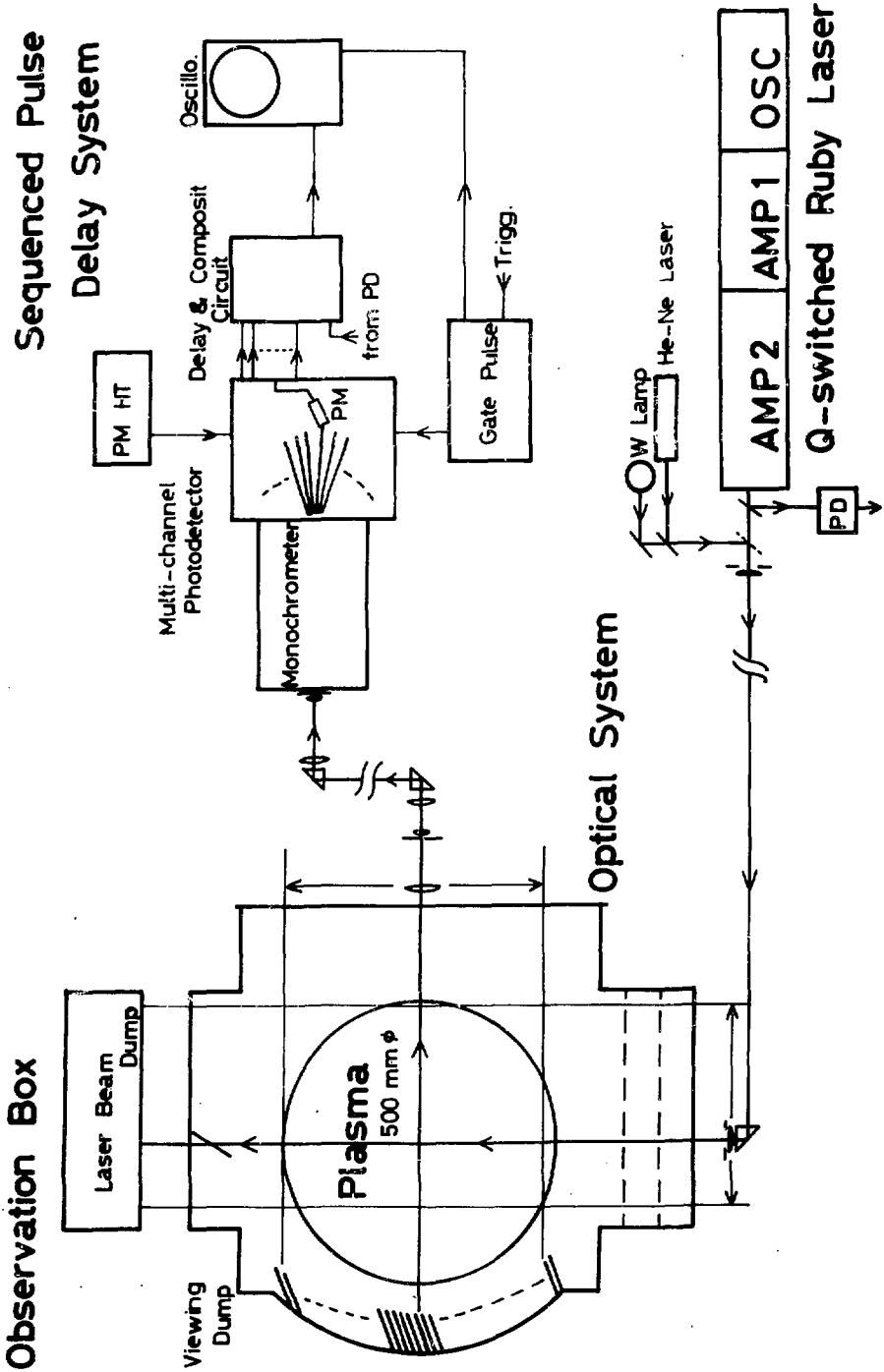


Fig. 2 Schematic diagram of ruby-laser scattering apparatus.[4)]

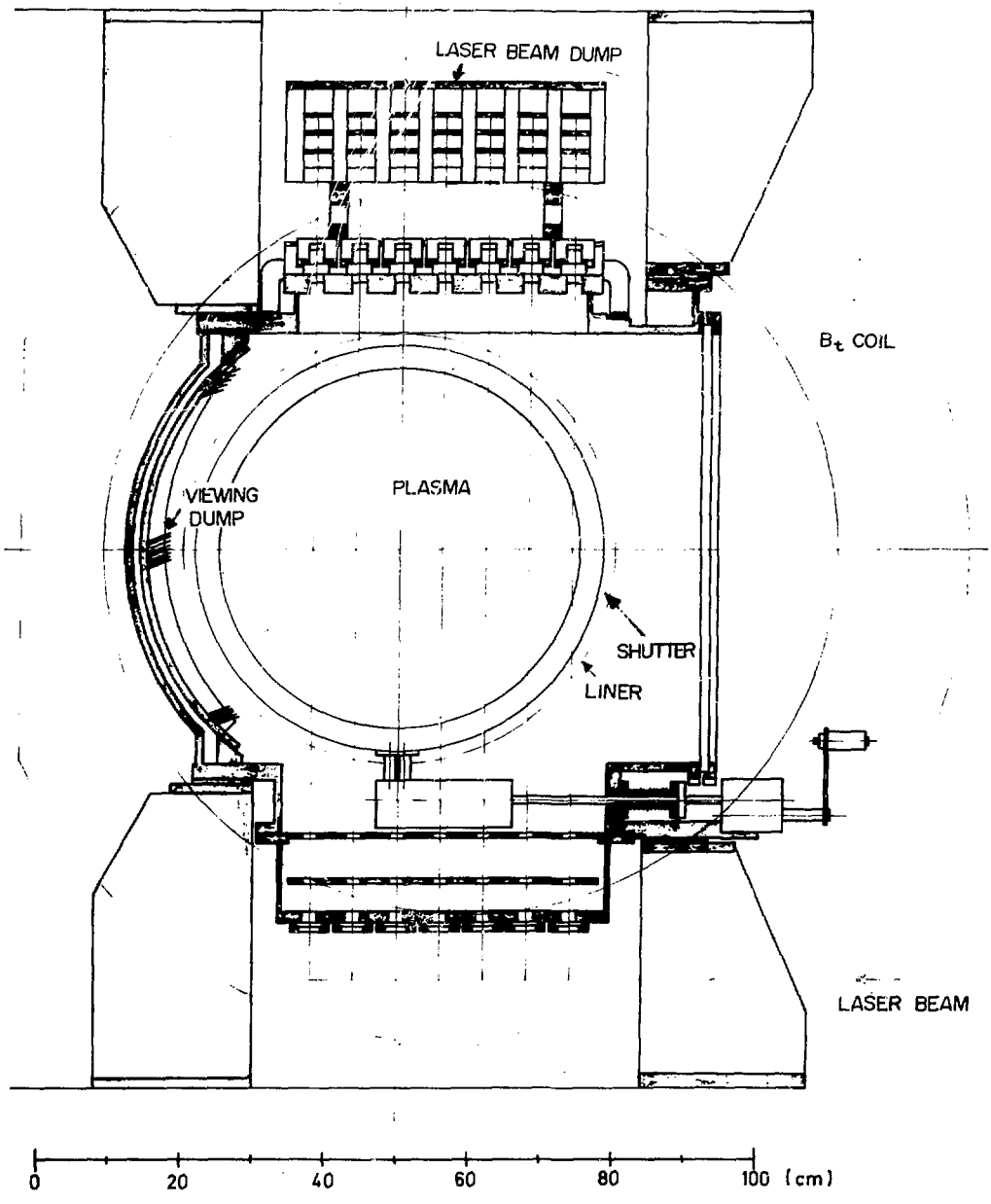


Fig. 3 Details of the observation port for ruby-laser scattering measurements.

## LASER SCATTERING

(i) Q-switched ruby laser

laser power --- 500 MW
pulse duration --- MAX 20 n sec
beam divergence --- MAX 5 m rad

(ii) Optical system

monochrometer ---Czerny-Turner mount, F6.5, f = 100 cm, grating 1200 lines/mm
focal spot size --- 3 mm at the center
horizontal scanning of laser light ---360 mm
vertical scanning of scattered light ---475 mm

(iii) Observation port

laser dump and viewing dump ---glass filter

(iv) Photodetector system

channel --- 12
photomultiplier --- RCA C31026
wavelength range per channel ---70 Å

(v) Sequenced pulse delay system

delay time between channels --- 50 n sec
gate width
slow gate --- 3 $\mu$ sec (PM)
fast gate --- 50 n sec (PM circuit)

Fig. 4 Main characteristics of ruby-laser scattering apparatus.

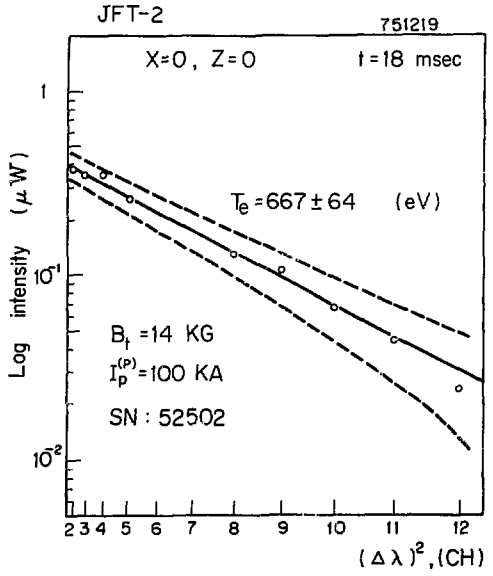


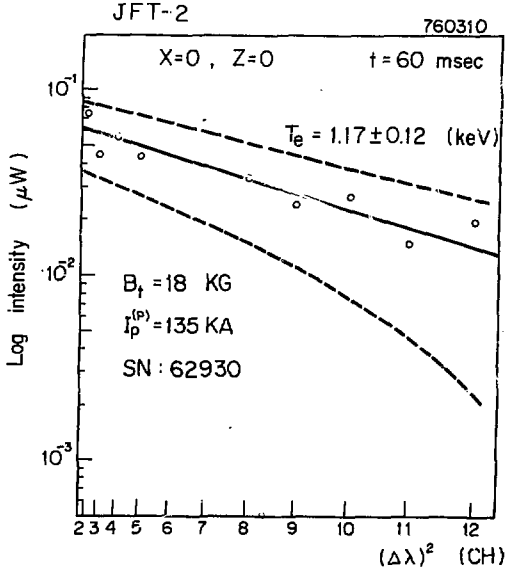


Fig. 5 Observed spectra of scattered lights from central plasmas.
(a) the toroidal magnetic field $B_t$ = 14 kG, peak plasma current $I_p(p)$ = 100 kA and t = 18 msec after a breakdown
(b) $B_p$ = 18 kG, $I_p(p)$ = 135 kA and t = 60 msec.

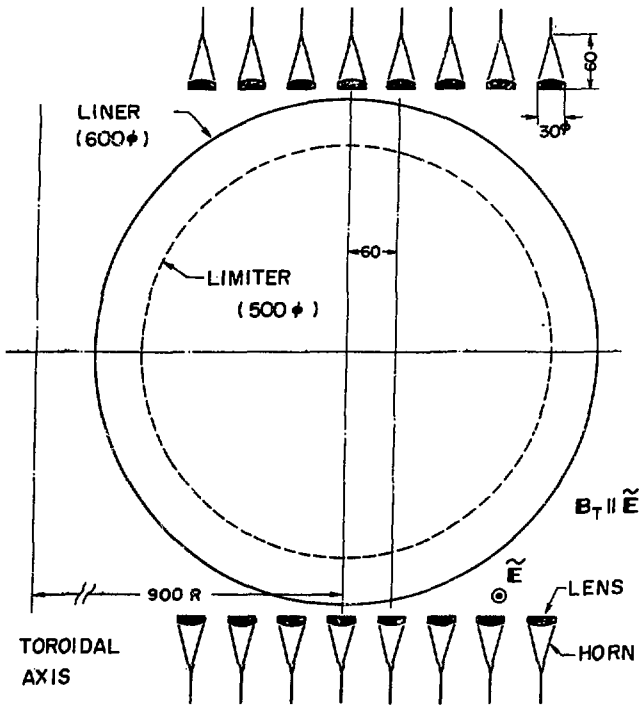


Fig. 6 Vertical paths for 4-mm wave interferometric measurements.

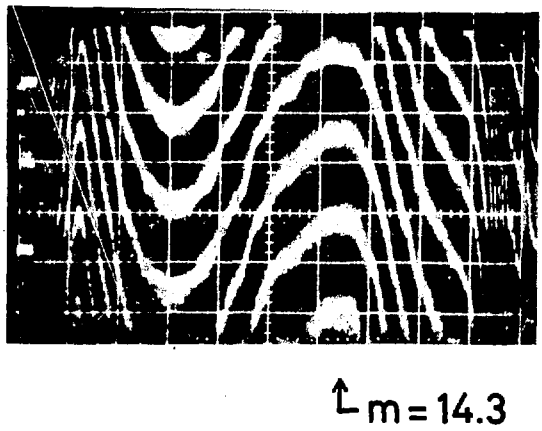


Fig. 7 Typical oscilloscopic trace of zebra-striped fringes observed with a 4-mm interferometer (time sweep 20 msec/div and $0.88 \times 10^{12}$ $cm^{-3}$ per fringe).

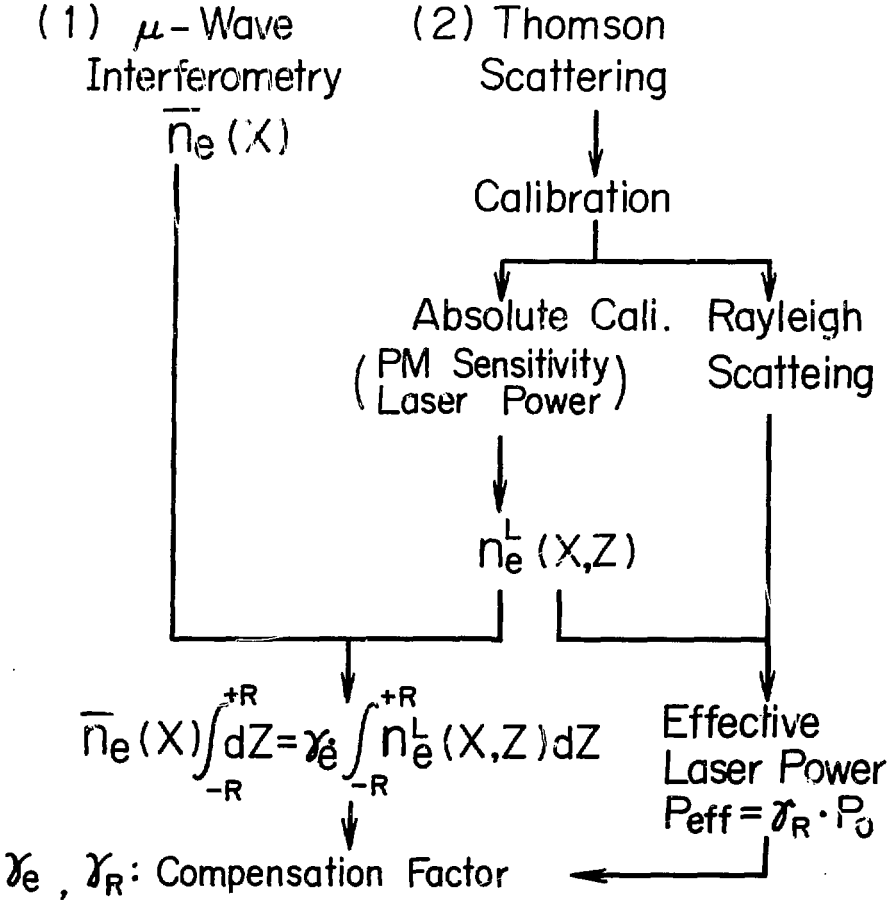


Fig. 8 Illustration of absolute calibrations in scattering measurements.

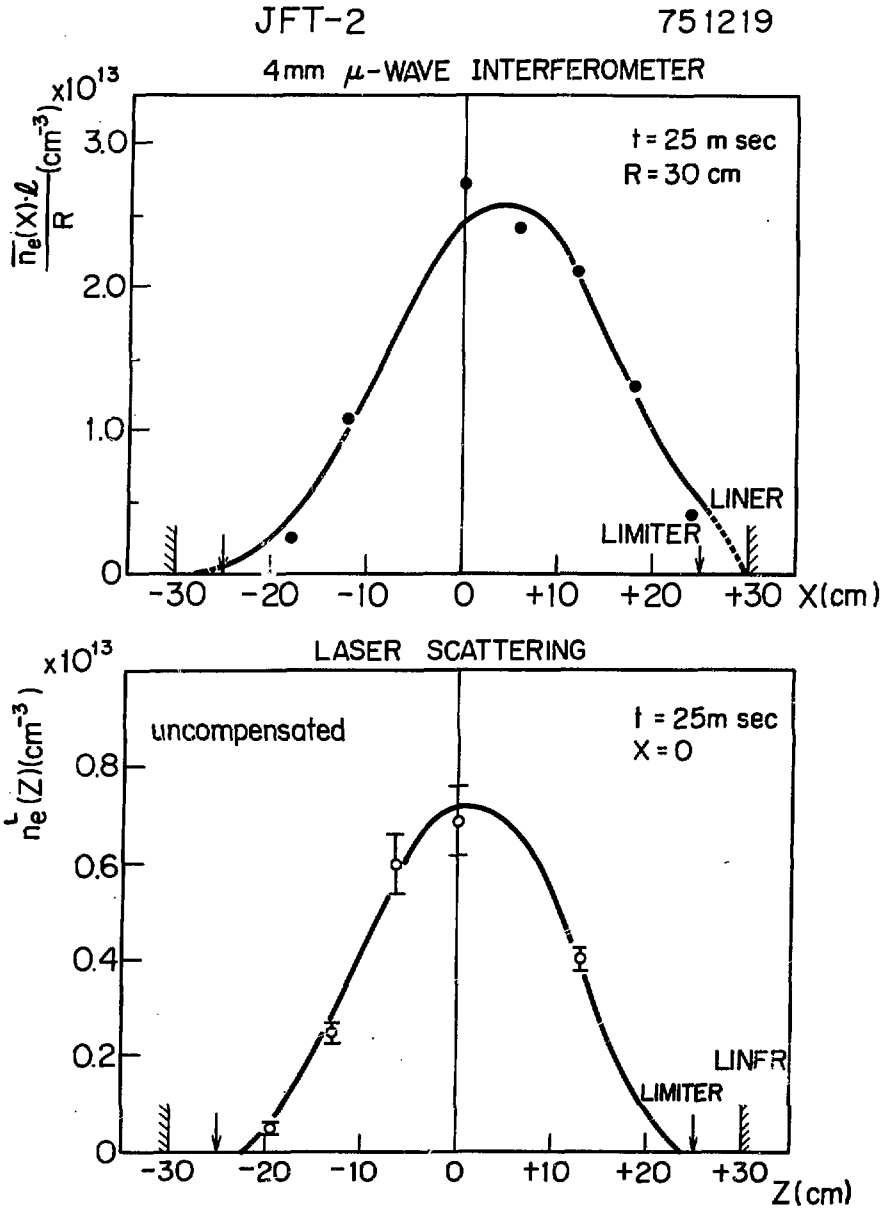


Fig. 9 Horizontal distribution of averaged electron density from 4-mm wave measurements (upper graph) and vertical distribution of apparent (uncompensated) electron density in a central, vertical plane from scattering measurements (lower graph).

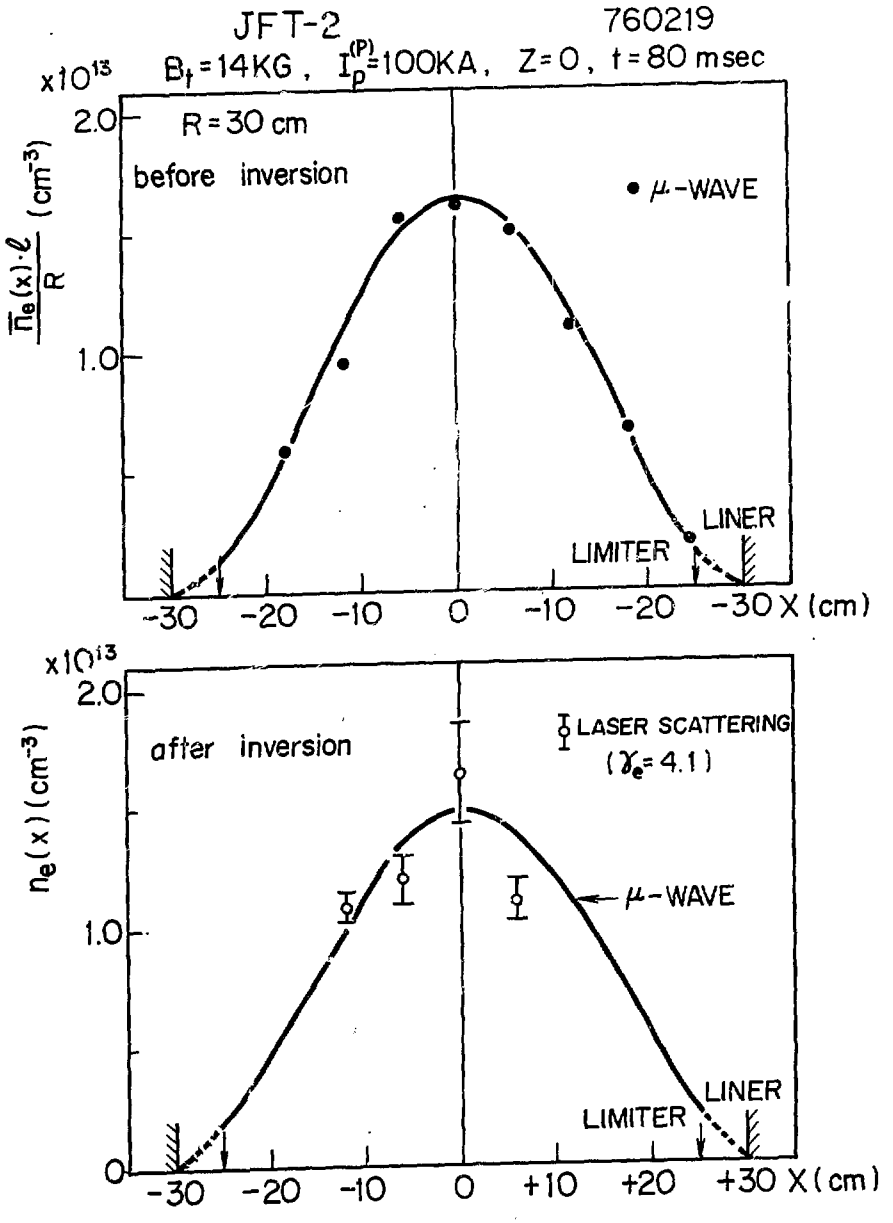


Fig.10(a) Comparison of horizontal density distribution between the two methods (lower graph) under $B_t$ = 14 kG, $I_p^{(p)}$ = 100 kA, and t = 80 msec. In the lower graph, the solid curve is determined through an inverse-transformation from the averaged densities (shown in the upper graph) measured with a 4-mm wave interferometer, and the open circles refer to the electron density multipled by a compensation factor $\gamma_e$ = 4.1 in ruby-laser scattering measurements.

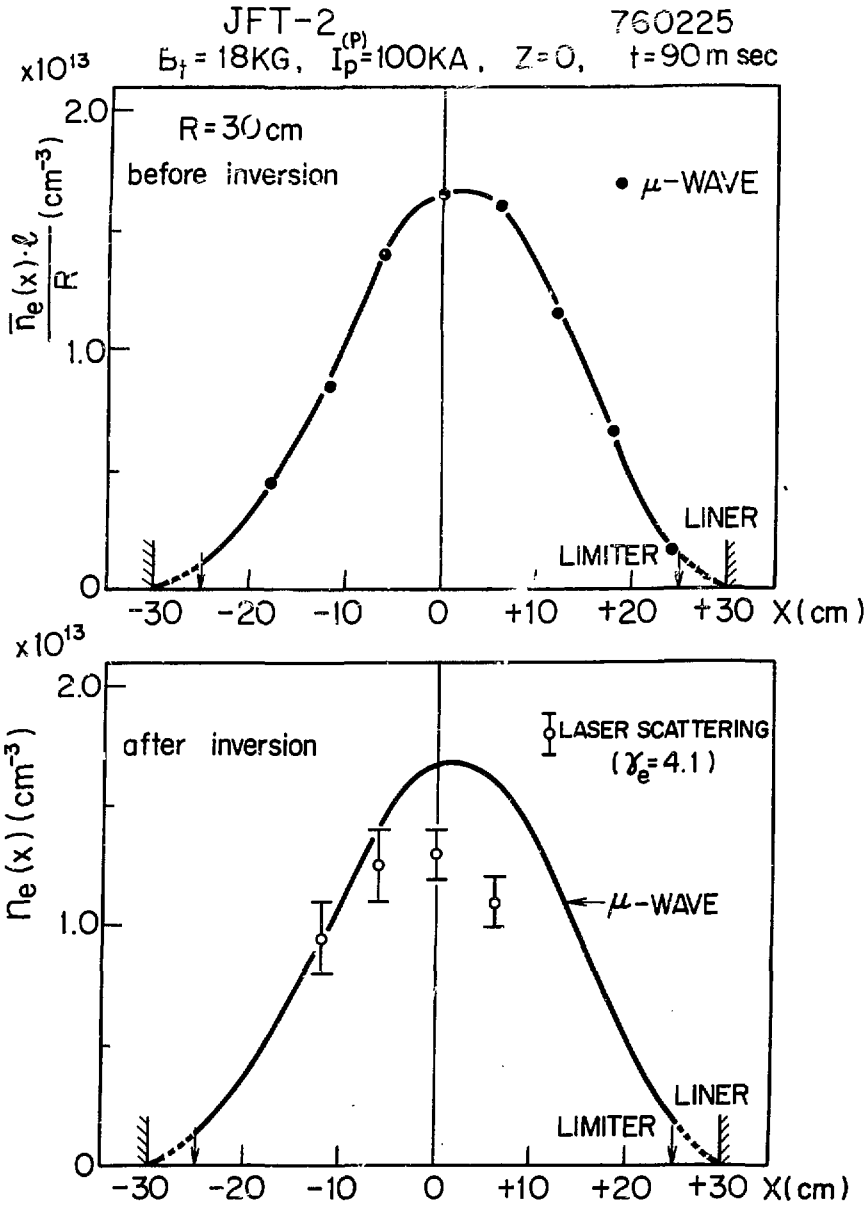


Fig.10(b) Comparison of horizontal density distribution between the two methods (lower graph) under $B_t$ = 18 kG, $I_p^{(p)}$ = 100 kA, and t = 90 msec.

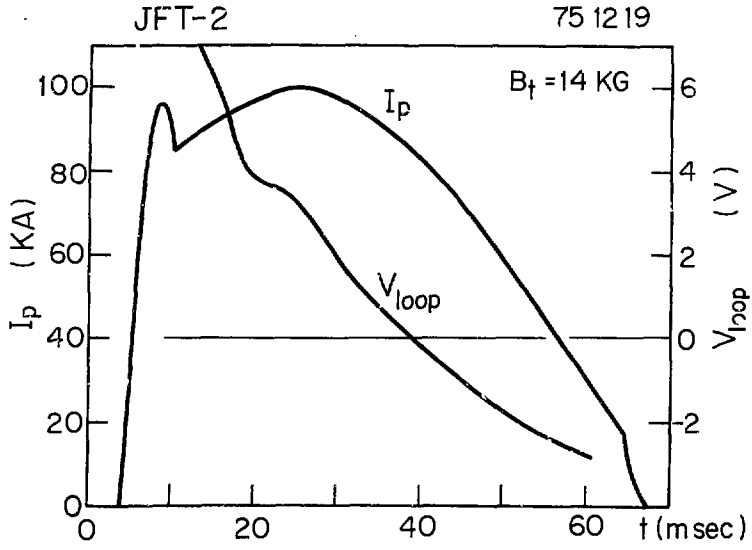


Fig. 11 Typical time-variations of the plasma current $I_p$ and loop voltage $V_{loop}$ under $B_t$ = 14 kG and $I_p^{(p)}$ = 100 kA.

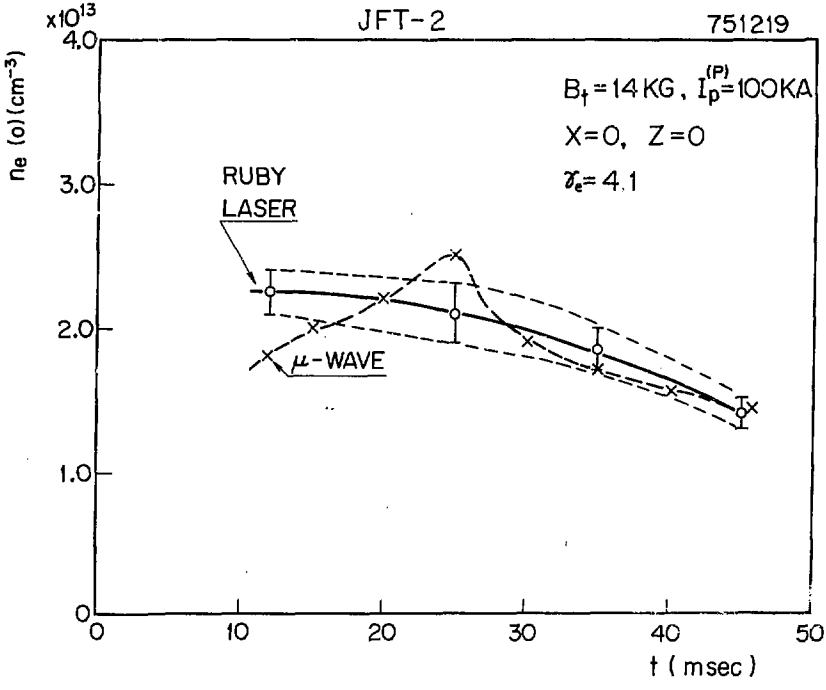


Fig. 13 Time-variations of central electron densities determined from ruby-laser scattering and 4-mm wave interferometric measurements.

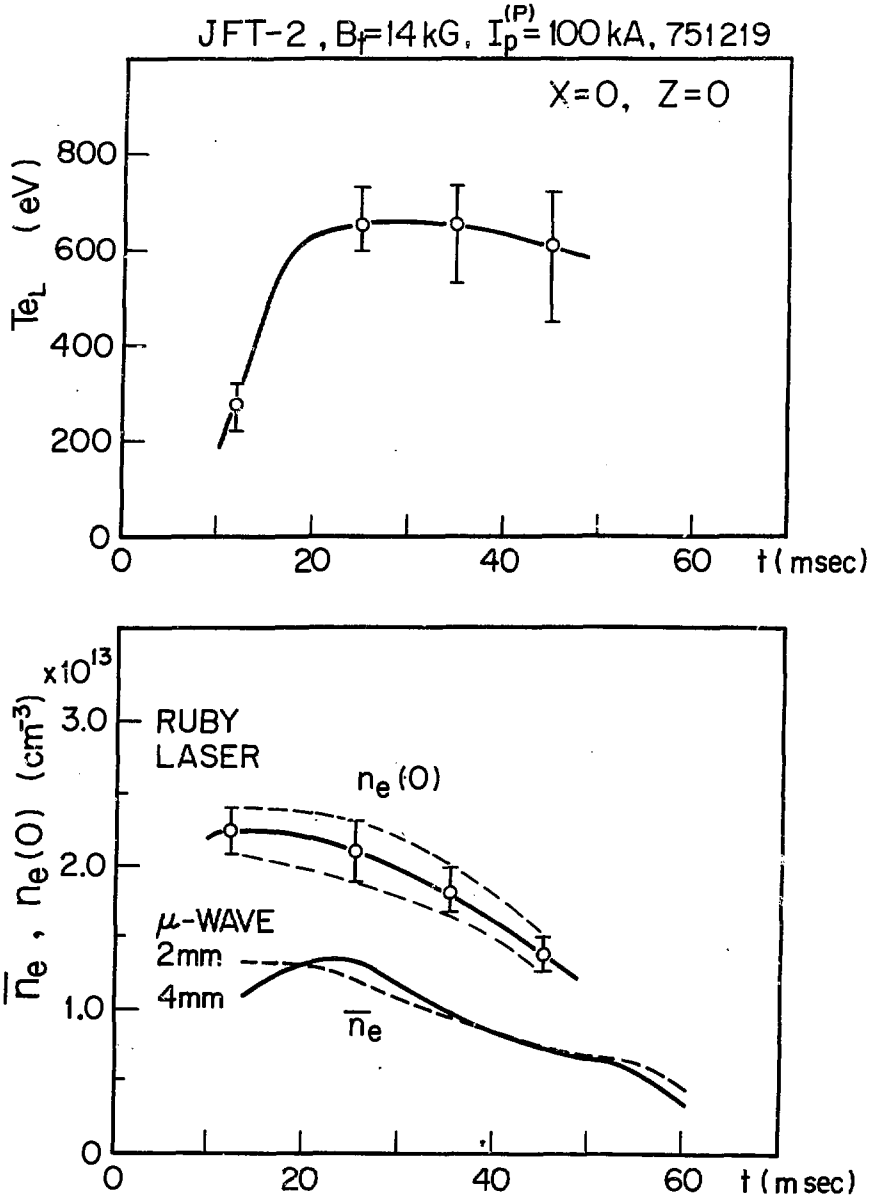


Fig. 12 Time-variations of central electron temperature $T_{eL}$ and density $n_e(0)$ and average electron density $\bar{n}_e$ under $B_t$ = 14 kG and $I_p^{(P)}$ = 100 kA.